FTU for heart wall

In this section we develop an sFTU representing a cylindrical tube segment of a pressure vessel such as the left ventricle, an artery, a tract of the digestive system, etc. The primary assumption is that the segment is thick-walled but undergoes simple kinematic deformations – axial extension, radial inflation and axial twist.

Axial extension, radial inflation and axial twist of a cylindrical tube

Consider the cylindrical tube shown in Figure 1(a).

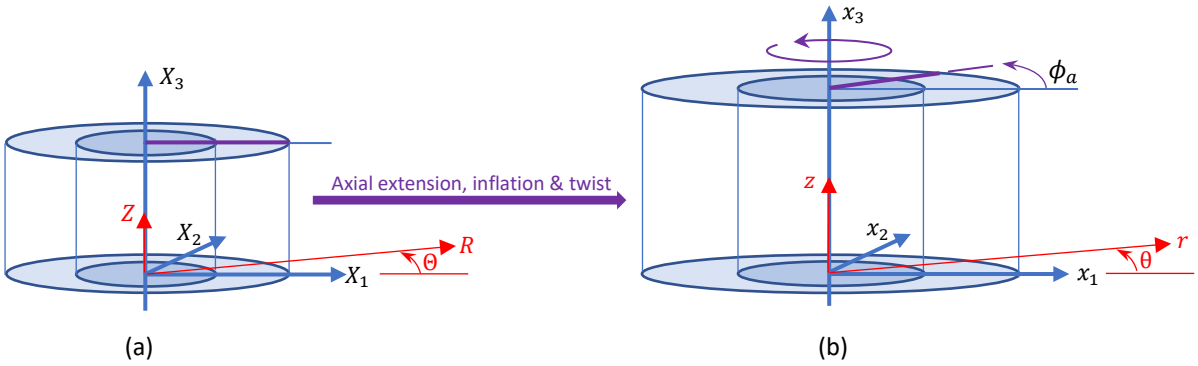

Figure 1 Coordinate systems for the cylinder in the (a) undeformed, and (b) deformed states. The cylinder is stretched axially by λ_a, inflated by $r = f(R)$ and twisted by ϕ radians per unit axial distance.

A point defined by material coordinates $(\nu_1, \nu_2, \nu_3,) \equiv (R, \Theta, \mathrm{Z})$ in the undeformed state has cartesian coordinates:

$$X_1 = R\cos\Theta$$
$$X_2 = R\sin\Theta$$
$$X_3 = Z$$

The gradient tensor $\frac{\partial X_i}{\partial \nu_\alpha} = \begin{bmatrix} \cos\Theta & -R\sin\Theta & 0 \\ \sin\Theta & R\cos\Theta & 0 \\ 0 & 0 & 1 \end{bmatrix}$

generates the metric tensors in the undeformed state:

$$A_{\alpha\beta} = \frac{\partial X_k}{\partial \nu_\alpha}\frac{\partial X_k}{\partial \nu_\beta} = \begin{bmatrix} 1 & 0 & 0 \\ 0 & R^2 & 0 \\ 0 & 0 & 1 \end{bmatrix};\quad A^{\alpha\beta} = \begin{bmatrix} 1 & 0 & 0 \\ 0 & R^{-2} & 0 \\ 0 & 0 & 1 \end{bmatrix};\quad A = \det A_{\alpha\beta} = R^2$$

We now consider the simultaneous extension, inflation and torsion of the cylindrical tube, defined by the cylindrically symmetric deformation

$$r = f(R)$$
$$\theta = \Theta + Z\phi_a$$
$$z = \lambda_a Z$$

in which a material point which is located at $(\nu_1, \nu_2, \nu_3) \equiv (R, \Theta, Z)$ in the undeformed state moves to the location (r, θ, z) in the deformed state. The deformation is defined by the axial extension ratio λ, the twist ϕ per unit of axial length, and the radial function $r = f(R)$, which will be chosen to ensure incompressibility of the tissue – no change in tube volume. Note that planes orthogonal to the axis of the tube are rotated about that axis and shifted in the z direction but remain as planes. We are also assuming that there is no shearing in the (r, θ)-plane.

The cartesian coordinates of the deformed state are:

$$x_1 = r\cos\theta = f(R).\cos\left(\Theta + Z\phi_a\right)$$
$$x_2 = r\sin\theta = f(R).\sin\left(\Theta + Z\phi_a\right)$$
$$x_3 = z = \lambda_a Z$$

Deformation gradient tensor

The deformation gradient tensor is therefore:

$$\frac{\partial x_i}{\partial \nu_\alpha} = \begin{bmatrix} \frac{dr}{dR}.\cos\theta & -r\sin\theta & -r\phi_a\sin\theta \\ \frac{dr}{dR}.\sin\theta & r\cos\theta & r\phi_a\cos\theta \\ 0 & 0 & \lambda_a \end{bmatrix};$$

giving the metric tensors in the deformed state

$$a_{\alpha\beta} = \frac{\partial x_k}{\partial \nu_\alpha}\frac{\partial x_k}{\partial \nu_\beta} = \begin{bmatrix} \left(\frac{dr}{dR}\right)^2 & 0 & 0 \\ 0 & r^2 & \phi_a r^2 \\ 0 & \phi_a r^2 & \lambda_a^2 + (r\phi_a)^2 \end{bmatrix};\ a = \det a_{\alpha\beta} = r^2\lambda_a^2\left(\frac{dr}{dR}\right)^2,$$

and

$$a^{\alpha\beta} = \begin{bmatrix} \left(\frac{dr}{dR}\right)^{-2} & 0 & 0 \\ 0 & r^{-2} + \left(\frac{\phi_a}{\lambda_a}\right)^2 & \frac{\phi_a}{\lambda_a^2} \\ 0 & \frac{\phi_a}{\lambda_a^2} & \lambda_a^{-2} \end{bmatrix};\ \det\ a^{\alpha\beta} = \frac{1}{a}. \tag{1}$$

Note on units: If r is in cm, a, a_{22} are cm^2, a_{23} is cm, a^{22} is cm^{-2} and a^{23} is cm^{-1} while a_{11}, a^{11}, a_{33} & a^{33} are dimensionless.

Imposing incompressibility

Incompressibility requires $a = A$ and hence

$$\left(\frac{dr}{dR}\right)^2 r^2\lambda_a^2 = R^2 \ \text{ or } \ \lambda_a\frac{r}{R}\frac{dr}{dR} = 1$$

or

$$\frac{dr}{dR} = \frac{R}{\lambda_a r}$$

and equation 1 becomes,

$$a^{\alpha\beta} = \begin{bmatrix} \left(\frac{\lambda_a r}{R}\right)^2 & 0 & 0 \\ 0 & r^{-2} + \left(\frac{\phi_a}{\lambda_a}\right)^2 & \frac{\phi_a}{\lambda_a^2} \\ 0 & \frac{\phi_a}{\lambda_a^2} & \lambda_a^{-2} \end{bmatrix}. \tag{2}$$

Integrating across the wall of the cylinder,

$$\lambda_a\int_{r_0}^{r} r\,dr = \int_{R_0}^{R} R\,dR\ ,$$

where R_0 and R are the inner and outer radii of the undeformed tube, and r_0 and r are the corresponding radii for the deformed tube.

Thus

$$\lambda_a(r^2 - r_0^2) = (R^2 - R_0^2)$$

which is consistent with no change on the volume of the cylinder.

Therefore, for any radius $R \geq R_0$, $r = f(R)$ is given by

$$r = \sqrt{r_0^2 + \lambda_a^{-1}(R^2 - R_0^2)}. \tag{3}$$

Green-Cauchy strain tensor

The Green strain tensor is

$$E_{\alpha\beta} = \tfrac{1}{2}\left(a_{\alpha\beta} - A_{\alpha\beta}\right) = \tfrac{1}{2}\begin{bmatrix} \left(\frac{R}{\lambda_a r}\right)^2 - 1 & 0 & 0 \\ 0 & r^2 - R^2 & \phi_a r^2 \\ 0 & \phi_a r^2 & \lambda_a^2 + (r\phi_a)^2 - 1 \end{bmatrix}. \tag{4}$$

Note on units: If r is in cm, E_{22} is cm^2 and E_{23} is cm, while E_{11} & E_{33} are dimensionless

Muscle fibre stretch

Now consider a muscle fibre embedded in the cylinder and lying in a plane of constant R in the undeformed state, moving to a plane of constant r in the deformed state, as illustrated in Figure 2.

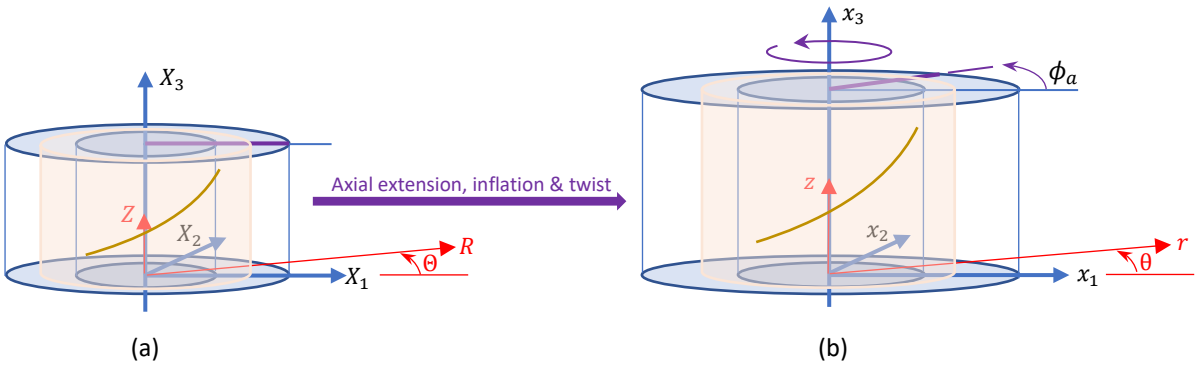

Figure 2. Deformation of a muscle fibre lying on a surface of constant radius.

Undeformed fibre

The cartesian coordinates of a material point lying on the fibre on a cylinder of radius R are given by

$$X_1 = R\cos(t\Theta_R)$$
$$X_2 = R\sin(t\Theta_R)$$
$$X_3 = t$$

where t is a normalised material parameter ($0 \le t \le 1$) that traces the change in circumferential angle from zero to Θ_R as the fibre winds around the cylinder of height $Z = 1$ (see Figure 3a).

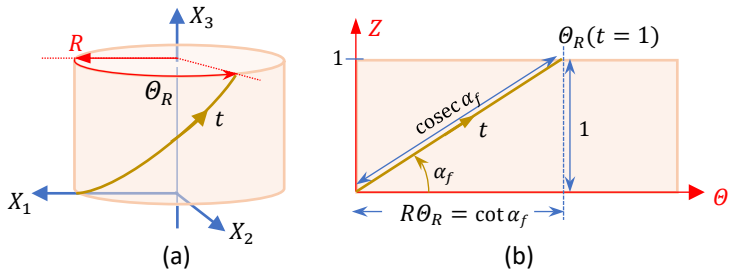

Figure 3. (a) A muscle fibre of fibre angle α_f lying on the undeformed cylindrical surface of radius R; (b) The unwrapped cylindrical surface. The length of the fibre is cosec α_f.

The fibre tangent is:

$$\boldsymbol{t} = \left\{\frac{\partial X_1}{\partial t}, \frac{\partial X_2}{\partial t}, \frac{\partial X_3}{\partial t}\right\} = \{-R\Theta_R\sin(t\Theta_R), R\Theta_R\cos(t\Theta_R), 1\},$$

or, normalised,

$$\hat{\boldsymbol{t}} = \{-R\Theta_R\sin(t\Theta_R), R\Theta_R\cos(t\Theta_R), 1\}/\sqrt{1 + (R\Theta_R)^2}.$$

The unit vector tangent to this surface in the X_1, X_2 plane at point t is:

$$\hat{\boldsymbol{s}} = \{-\sin(t\Theta_R), \cos(t\Theta_R), 0\},$$

and the angle between $\hat{\boldsymbol{t}}$ and $\hat{\boldsymbol{s}}$ is therefore (using $R\Theta_R = \cot\alpha_f$)

$$\cos^{-1}(\hat{\boldsymbol{t}}.\hat{\boldsymbol{s}}) = \cos^{-1}\left(\frac{R\Theta_R}{\sqrt{1+(R\Theta_R)^2}}\right) = \cos^{-1}\left(\frac{\cot\alpha_f}{\sqrt{1+\cot^2\alpha_f}}\right) = \alpha_f\,,$$

as expected. Note that the cartesian coordinates of a point t on the fibre at a radius of R are:

$$X_1 = R\cos(t\Theta_R) = R\cos\left(t\frac{\cot\alpha_f}{R}\right)$$
$$X_2 = R\sin t\Theta_R = R\sin\left(t\frac{\cot\alpha_f}{R}\right)$$
$$X_3 = t$$

In the undeformed state, the length of the fibre lying within the cylindrical surface is:

$$\int_{t=0}^{t=1}\sqrt{\left(\frac{\partial X_1}{\partial t}\right)^2+\left(\frac{\partial X_2}{\partial t}\right)^2+\left(\frac{\partial X_3}{\partial t}\right)^2}\,.dt = \int_{t=0}^{t=1}\sqrt{1+\cot^2\alpha_f}\,.dt = \operatorname{cosec}\alpha_f \qquad (5)$$

as shown in Figure 3(b).

Deformed fibre

Figure 4 shows the change in fibre length for inflation ($R \to r$), axial extension (ratio λ_a) and twist (ϕ_a).

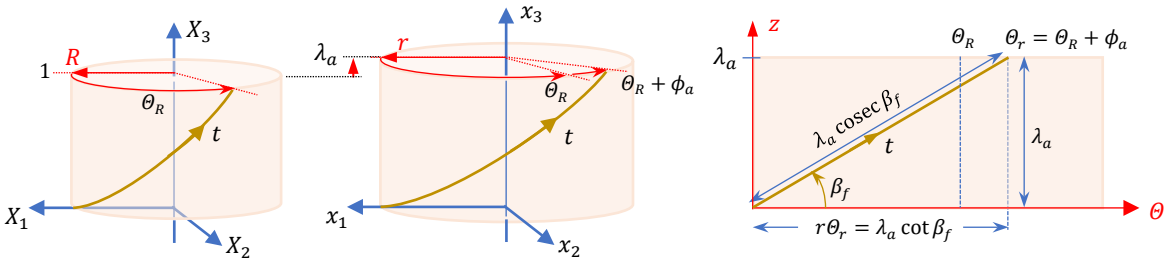

(a) (b) (c)

Figure 4. Fibre deformation: (a) Undeformed muscle fibre of fibre angle α lying on the undeformed cylindrical surface of radius R; (b) The same fibre lying on the deformed surface which is inflated to radius r, extended axially by λ_a, and twisted through angle ϕ_a; (c) The fibre appears as a straight line on the cylindrical surface.

In the deformed state,

$$x_1 = r\cos t\Theta_r$$
$$x_2 = r\sin t\Theta_r$$
$$x_3 = \lambda_a t$$

and, from Figure 4(c),

$$r\Theta_r = \lambda_a\cot\beta_f$$

giving the deformed fibre angle β_f in terms of the angle α_f used to define the undeformed fibre:

$$\beta_f = \cot^{-1}\left(\frac{r\Theta_r}{\lambda_a}\right)$$

The length of the deformed fibre is:

$$\int_{t=0}^{t=1}\sqrt{\left(\frac{\partial x_1}{\partial t}\right)^2+\left(\frac{\partial x_2}{\partial t}\right)^2+\left(\frac{\partial x_3}{\partial t}\right)^2}\,.dt = \sqrt{(r\Theta_r)^2+\lambda_a^2} = \lambda_a\sqrt{1+\cot^2\beta_f} = \lambda_a\operatorname{cosec}\beta_f,$$

as shown in Figure 4(c). The fibre stretch ratio is therefore

$$\lambda_f = \frac{\lambda_a\operatorname{cosec}\beta_f}{\operatorname{cosec}\alpha_f} = \lambda_a\sin\alpha_f\operatorname{cosec}\beta_f,$$

where

$$\lambda_a \operatorname{cosec} \beta_f = \sqrt{\lambda_a^2 + (r\Theta_r)^2} = \sqrt{\lambda_a^2 + r^2\left(\Theta_R + \phi_a\right)^2} = \sqrt{\lambda_a^2 + r^2\left(\frac{\cot \alpha_f}{R} + \phi_a\right)^2}.$$

Therefore

$$\lambda_f = \sin \alpha_f \sqrt{\lambda_a^2 + r^2\left(\frac{\cot \alpha_f}{R} + \phi_a\right)^2},$$

and using equation 1 ($r = \sqrt{r_0^2 + \lambda_a^{-1}(R^2 - R_0^2)}$ – ensuring incompressibility),

$$\lambda_f = \sin \alpha_f \sqrt{\lambda_a^2 + \left(r_0^2 + \lambda_a^{-1}(R^2 - R_0^2)\right)\left(\frac{\cot \alpha_f}{R} + \phi_a\right)^2}$$

or

$$\lambda_f = \sqrt{\lambda_a^2 \sin^2 \alpha_f + \left(r_0^2 + \lambda_a^{-1}(R^2 - R_0^2)\right)\left(\frac{\cos \alpha_f}{R} + \phi_a \sin \alpha_f\right)^2}. \quad (6)$$

This equation provides the relationship, at any radial position R, between the fibre angle (α_f), the three parameters (r_0, λ_a, ϕ_a) defining the deformation of the incompressible thick-walled cylinder, and the resulting fibre stretch λ_f.

Simplified cases

When $\alpha_f = 0$, equation 6 becomes

$$\lambda_f = \frac{1}{R}\sqrt{r_0^2 + \lambda_a^{-1}(R^2 - R_0^2)} = \frac{r}{R}$$

which is independent of axial twist, as expected (see Figure 5).

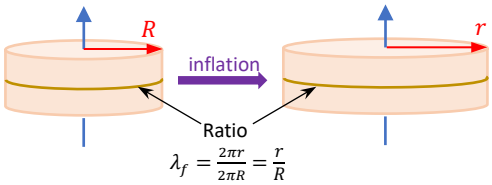

Figure 5 The simplest case: deformation of a circumferential muscle fibre lying on a surface of constant radius.

With no axial twist ($\phi_a = 0$) and no axial stretch ($\lambda_a = 1$), equation 6 becomes

$$\lambda_f = \sqrt{\sin^2 \alpha_f + \left(r_0^2 + (R^2 - R_0^2)\right)\left(\frac{\cos \alpha_f}{R}\right)^2}.$$

Transmurally varying fibre angle

Now consider a range of fibre angles across the wall thickness, as illustrated in Figure 6.

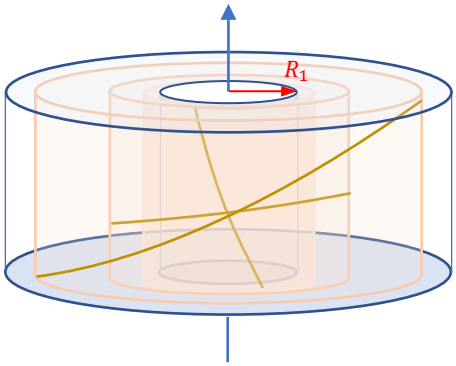

Figure 6 Fibres with varying angles shown at three different depths through the wall in the undeformed state.

Results (using OpenCOR []) are shown in Figure 7a for a cylinder of initial inner radius $R_0 = 1$ expanded to $r_0 = 1.2$ with no axial extension or rotation. The fibres are circumferential and there is a fall off in fibre extension ratio from $\lambda_f = \frac{r}{R} = 1.2$ at $R = 1$ to $\lambda_f = \frac{r}{R} = 1.0536$ at the outer wall $R = 2$ (where $r = \sqrt{1.2^2 + 3} = 2.107$) – a range of fibre extension of about $\boldsymbol{\Delta\lambda_a = 0.15}$. In Figure 7(b) the fibre angle is

set to vary linearly across the wall from $\alpha_f = 90\text{deg}$ at the inner wall to $\alpha_f = -60\text{deg}$ at the outer wall (results labelled with $\lambda_a = 1$). Note that this transmural fibre distribution produces a smaller range of fibre stretch ($\boldsymbol{\Delta\lambda_a = 0.09}$). When the cylinder is also extended axially with $\lambda_a = 1.1$, the range of fibre stretch is further reduced ($\boldsymbol{\Delta\lambda_a = 0.06}$). Finally, applying an additional axial twist of ϕ_a = -1.15deg further reduces the range of fibre stretch to $\boldsymbol{\Delta\lambda_a = 0.04}$ (i.e. a four-fold reduction in the variation of myofilament stretch ratio is achieved with a combination axial extension and twist combined with transmural fibre angle variation).

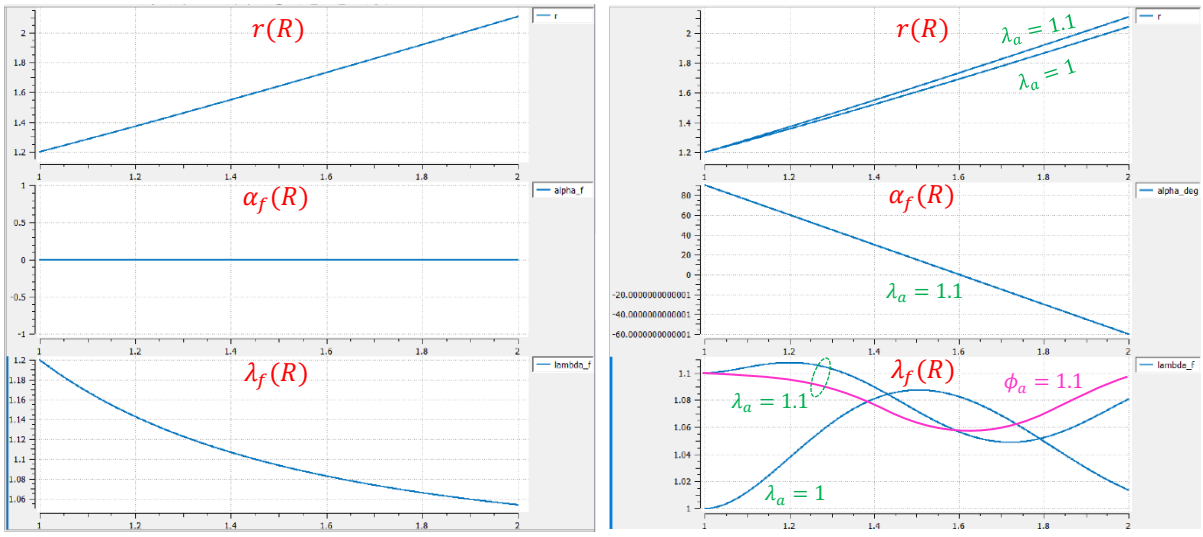

(a) (b)

Figure 7 From top to bottom: $r(R)$, $\alpha_f(R)$, $\lambda_f(R)$ for (a) $\alpha_f = 0, \lambda_a = 1, \phi_a = 0$; (b) α_f = +90deg to -60deg, for three loading configurations: (i) $\lambda_a = 1, \phi_a = 0$, (ii) $\lambda_a = 1.1, \phi_a = 0$, and (iii) $\lambda_a = 1.1, \phi_a = -0.02$ (-1.15deg).

Stress tensors

There are three alternative stress tensors commonly used in continuum mechanics. The Cauchy stress tensor $\widehat{\boldsymbol{T}} = \left\{\hat{T}^{ij}\right\}$ (symmetric) has physically meaningful components which are defined as force per unit area of the current deformed body and are referred to local cartesian coordinates $(\hat{x}_1, \hat{x}_2, \hat{x}_3)$. The 2nd Piola-Kirchhoff stress tensor $\boldsymbol{T} = \{T^{\alpha\beta}\}$ is used in defining constitutive equations since it defines stress as a force per unit area of the undeformed body (needed because the strains are relative to the undeformed body). The 2nd P-K stress tensor is also symmetric and invariant to rigid body rotation. In this application it has components that refer to the material coordinates (v_1, v_2, v_3) that are chosen to coincide with (R, Θ, Z) in the undeformed body and (r, θ, z) in the deformed body. A third, the 1st Piola-Kirchhoff stress tensor, is part way between these two as it defines components with respect to the undeformed areas but aligns the component directions with the deformed state and in general is not symmetric. However, in the present cylindrical coordinate configuration it is the same as the 2nd Piola-Kirchhoff stress tensor.

The relationship between the Cauchy and 2nd Piola-Kirchhoff stress tensors is given by

$$\widehat{\boldsymbol{T}} = \frac{\rho}{\rho_0}\boldsymbol{F}\boldsymbol{T}\boldsymbol{F}^T \quad \text{or} \quad \hat{T}^{ij} = \frac{\rho}{\rho_0}\frac{\partial \hat{x}_i}{\partial v_\alpha}T^{\alpha\beta}\frac{\partial \hat{x}_j}{\partial v_\beta},$$

where

$$\boldsymbol{F} = \frac{\partial \hat{x}_i}{\partial v_\alpha} = \begin{bmatrix} 1 & 0 & 0 \\ 0 & r & 0 \\ 0 & 0 & 1 \end{bmatrix}$$

and ρ and ρ_0 are the material densities of the deformed and undeformed body. For incompressible materials, $\rho = \rho_0$.

Strain energy density

Soft biological tissue exhibits 'strain stiffening': as the tissue is stretched, the amount of energy per unit volume needed to achieve another equal increment of stretch in that direction increases []. The same highly nonlinear behaviour is seen with a shearing deformation. The initial strain energy is typically very small at low strain and asymptotes to a limiting strain beyond which the tissue is damaged. Some hysteresis is also present, but this is very small for cardiac tissue.

Soft biological tissues are seldom isotropic, are occasionally transversely isotropic, but are more generally orthotropic (the properties are different in three orthogonal directions). Here we assume orthotropy and assume that the total strain energy density W is the sum of energy terms associated with stretching and shearing in the material coordinates (v_1, v_2, v_3) mentioned above.

These three characteristics of strain stiffening, orthotropy and strain mode independence are captured with the following 'pole-zero' strain energy density function []:

$$W = \sum_{\alpha\beta} W(E_{\alpha\beta}) \quad \text{(J.L}^{-1}\text{)},$$

where

$$W(E_{\alpha\beta}) = \frac{k_{\alpha\beta}}{2c_{\alpha\beta}} \cdot \frac{E_{\alpha\beta}^2}{(c_{\alpha\beta} - |E_{\alpha\beta}|)^2}, \text{ (no summation on } \alpha, \beta\text{)}, \tag{7}$$

as illustrated in Figure 8a, and where the Green strain tensor $E_{\alpha\beta}$ is given by equation 4.

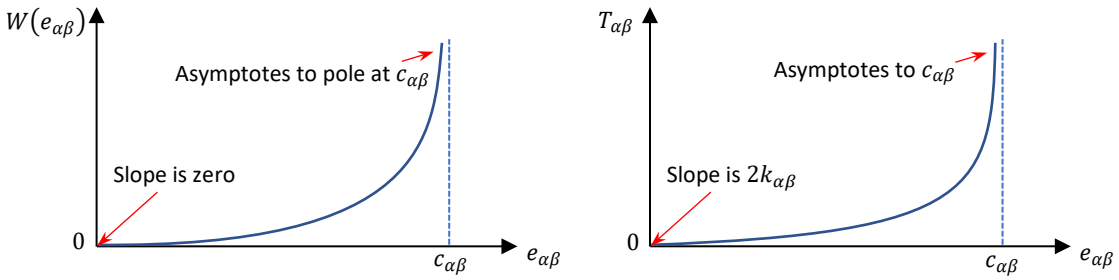

(a) (b)

Figure 8 The strain stiffening behaviour characteristic of soft biological tissue, showing asymptotic behaviour (to a 'pole' at $E_{\alpha\beta} = c_{\alpha\beta}$). (a) The strain energy density; and (b) the 2nd Piola-Kirchhoff stress.

The contravariant 2nd Piola-Kirchhoff stress tensor $\boldsymbol{T} = \{T^{\alpha\beta}\}$ is obtained from the strain energy density as

$$T^{\alpha\beta} = \frac{\partial W}{\partial E_{\alpha\beta}} + pa^{\alpha\beta} + T_0 a_1^\alpha a_1^\beta = \frac{\partial W(E_{\alpha\beta})}{\partial E_{\alpha\beta}} + pa^{\alpha\beta} + T_0 a_1^\alpha a_1^\beta \tag{8}$$

where p is the hydrostatic pressure (for the assumed incompressible material) and T_0 is an actively generated myofilament stress that lies in the fibre direction η_1(see below). Substituting (7) into (8),

$$T^{\alpha\beta} = \frac{k_{\alpha\beta}}{c_{\alpha\beta}} \left(\frac{E_{\alpha\beta}}{(c_{\alpha\beta} - |E_{\alpha\beta}|)^2} + \frac{E_{\alpha\beta}^2}{(c_{\alpha\beta} - |E_{\alpha\beta}|)^3} \right) + pa^{\alpha\beta} + T_0 a_1^\alpha a_1^\beta$$

or

$$T^{\alpha\beta} = k_{\alpha\beta} \frac{E_{\alpha\beta}}{(c_{\alpha\beta} - |E_{\alpha\beta}|)^3} + pa^{\alpha\beta} + T_0 a_1^\alpha a_1^\beta \tag{9}$$

Note on units: If r is in cm (consistent with volume in litres), then

- k_{11}, T^{11}, p, T_0 are J.L^{-1} (=kPa)
- c_{22}, E_{22} are cm^2; k_{22} is J.L^{-1}.cm^2; a^{22} is cm^{-2}; T^{22} is J.L^{-1}.cm^{-2}
- k_{33}, T^{33} are J.L^{-1}
- c_{23}, E_{23} are cm; k_{23} is J.L^{-1}.cm; a^{23} is cm^{-1}; T^{23} is J.L^{-1}.cm^{-1}
- all other quantities are dimensionless

With incompressibility,

$$E_{\alpha\beta} = \frac{1}{2}\begin{bmatrix} \left(\frac{R}{\lambda_a r}\right)^2 - 1 & 0 & 0 \\ 0 & r^2 - R^2 & \phi_a r^2 \\ 0 & \phi_a r^2 & \lambda_a^2 + (r\phi_a)^2 - 1 \end{bmatrix}. \tag{10}$$

Note that since the fibre axis varies transmurally and does not align with any wall coordinate axes, T_0 must be transformed by the mixed metric tensor

$$a_1^\alpha = \frac{\partial \nu_\alpha}{\partial \eta_1}$$

where $(\nu_1, \nu_2, \nu_3,) \equiv (R, \Theta, Z)$ are the wall material coordinates and η_1 is the fibre direction material coordinate defined in the undeformed reference state. Since the fibres lie in the (Θ, Z) plane, this is in fact given by (see Figure 3b)

$$a_1^\alpha = \frac{\partial \nu_\alpha}{\partial \eta_1} = \left(0, \frac{1}{r}\cos\alpha_f, \sin\alpha_f\right) \quad \text{(or } \beta_f \text{ depending on how we define } T_0\text{)},$$

and hence

$$a_1^\alpha a_1^\beta = \begin{bmatrix} 0 & 0 & 0 \\ 0 & \frac{1}{r^2}\cos^2\alpha_f & \frac{1}{r}\cos\alpha_f \sin\alpha_f \\ 0 & \frac{1}{r}\cos\alpha_f \sin\alpha_f & \sin^2\alpha_f \end{bmatrix}. \tag{11}$$

The hydrostatic pressure term p (effectively the Lagrange multiplier on the incompressibility condition) must be determined from stress boundary conditions. In a transmural sense these are the left ventricular pressure (inner surface) and zero traction at the epicardial boundary (outer surface).

Actively generated stress

We now consider the T_0 term in equation 9, representing the contribution to force balance of a stress that is generated by myofilament cross-bridges. The relationship of this term to fibre extension ratio and its velocity is considered in detail below, but we first explore the consequences of imposing a constant value of T_0.

Stress equilibrium

The 2nd Piola-Kirchhoff stress tensor

$$T^{\alpha\beta} = \begin{bmatrix} T^{rr} & 0 & 0 \\ 0 & T^{\theta\theta} & T^{\theta z} \\ 0 & T^{z\theta} & T^{zz} \end{bmatrix} = \begin{bmatrix} \frac{\partial W}{\partial E_{rr}} & 0 & 0 \\ 0 & \frac{\partial W}{\partial E_{\theta\theta}} & \frac{\partial W}{\partial E_{\theta z}} \\ 0 & \frac{\partial W}{\partial E_{z\theta}} & \frac{\partial W}{\partial E_{zz}} \end{bmatrix} + p\begin{bmatrix} \left(\frac{\lambda_a r}{R}\right)^2 & 0 & 0 \\ 0 & r^{-2} + \left(\frac{\phi_a}{\lambda_a}\right)^2 & \frac{\phi_a}{\lambda_a^2} \\ 0 & \frac{\phi_a}{\lambda_a^2} & \lambda_a^{-2} \end{bmatrix} + T_0\begin{bmatrix} 0 & 0 & 0 \\ 0 & \frac{1}{r^2}\cos^2\alpha_f & \frac{1}{r}\cos\alpha_f \sin\alpha_f \\ 0 & \frac{1}{r}\cos\alpha_f \sin\alpha_f & \sin^2\alpha_f \end{bmatrix},$$

has three direct stress components (in the (r, θ, z)-directions), but only one shear stress ($T^{\theta z} = T^{z\theta}$).

The Cauchy stress tensor is

$$\hat{T}^{ij} = \begin{bmatrix} \frac{\partial W}{\partial E_{rr}} & 0 & 0 \\ 0 & r^2\frac{\partial W}{\partial E_{\theta\theta}} & r\frac{\partial W}{\partial E_{\theta z}} \\ 0 & r\frac{\partial W}{\partial E_{z\theta}} & \frac{\partial W}{\partial E_{zz}} \end{bmatrix} + p\begin{bmatrix} \left(\frac{\lambda_a r}{R}\right)^2 & 0 & 0 \\ 0 & 1 + \left(\frac{r\phi_a}{\lambda_a}\right)^2 & \frac{r\phi_a}{\lambda_a^2} \\ 0 & \frac{r\phi_a}{\lambda_a^2} & \lambda_a^{-2} \end{bmatrix} + T_0\begin{bmatrix} 0 & 0 & 0 \\ 0 & \cos^2\alpha_f & \cos\alpha_f \sin\alpha_f \\ 0 & \cos\alpha_f \sin\alpha_f & \sin^2\alpha_f \end{bmatrix}, \tag{12}$$

Note that W, p and T_0 all have units of J.L^{-1} (energy density or force per unit area).

Stress equilibrium is ensured by $\nabla.\hat{\boldsymbol{T}} = 0$ [Malvern]. Note that λ_a and ϕ_a are constants and α_f varies radially. All components of stress vary radially but not in the circumferential or axial directions. Since the only stress gradients are in the radial direction, the only equilibrium equation that needs to be considered is

$$\frac{1}{r}\frac{d}{dr}\left(r\hat{T}^{rr}\right) - \frac{1}{r}\hat{T}^{\theta\theta} = 0\,, \quad \text{or } \frac{d}{dr}\left(r\hat{T}^{rr}\right) = \hat{T}^{\theta\theta}\,,$$

and hence

$$\frac{d}{dr}\left[r\frac{\partial W}{\partial E_{rr}}+pr^3\frac{\lambda_a^2}{R^2}\right]=r^2\frac{\partial W}{\partial E_{\theta\theta}}+p\left[1+\frac{\phi_a^2}{\lambda_a^2}r^2\right]+T_0\cos^2\alpha_f\,, \tag{13}$$

where

$$\frac{\partial W}{\partial E_{rr}}=\frac{k_{rr}.E_{rr}}{(c_{rr}-|E_{rr}|)^3},\quad \text{with}\quad E_{rr}=\frac{1}{2}\left[\left(\frac{R}{\lambda_a r}\right)^2-1\right], \tag{14}$$

$$\frac{\partial W}{\partial E_{\theta\theta}}=\frac{k_{\theta\theta}.E_{\theta\theta}}{(c_{\theta\theta}-|E_{\theta\theta}|)^3},\quad \text{with}\quad E_{\theta\theta}=\frac{1}{2}(r^2-R^2), \tag{15}$$

Note the two boundary conditions on $\hat{T}^{rr}$:

$$\hat{T}^{rr}\big|_{r=r_{endo}}=-p_{LV}\ \text{ and }\ \hat{T}^{rr}\big|_{r=r_{epi}}=0. \tag{16}$$

Note that W, p and T_0 all have units of J.m^{-3} (energy density).

Expanding (13),

$$\frac{\partial W}{\partial E_{rr}}+r\frac{d}{dr}\left(\frac{\partial W}{\partial E_{rr}}\right)+r^3\frac{\lambda_a^2}{R^2}\frac{dp}{dr}+p\lambda_a^2\left(\frac{3r^2}{R^2}-\frac{2r^3}{R^3}\frac{dR}{dr}\right)=r^2\frac{\partial W}{\partial E_{\theta\theta}}+p\left[1+\left(\frac{r\phi_a}{\lambda_a}\right)^2\right]+T_0\cos^2\alpha_f\,,$$

or

$$\frac{dp}{dr}=\frac{R^2}{r^3\lambda_a^2}\left\{p\left[1+\left(\frac{r\phi_a}{\lambda_a}\right)^2-\lambda_a^2\left(\frac{3r^2}{R^2}-\frac{2r^3}{R^3}\frac{dR}{dr}\right)\right]+r^2\frac{\partial W}{\partial E_{\theta\theta}}-\frac{\partial W}{\partial E_{rr}}-r\frac{d}{dr}\left(\frac{\partial W}{\partial E_{rr}}\right)+T_0\cos^2\alpha_f\right\},$$

where the incompressibility condition (3)

$$R^2=R_0^2+\lambda_a(r^2-r_0^2)$$

gives

$$2R\frac{dR}{dr}=2\lambda_a r\quad\text{or}\quad\frac{dR}{dr}=\lambda_a\frac{r}{R}.$$

Therefore

$$\frac{dp}{dr}=\frac{R^2}{r^3\lambda_a^2}\left\{p\left[1+\left(\frac{r\phi_a}{\lambda_a}\right)^2-\lambda_a^2\left(\frac{3r^2}{R^2}-\frac{2\lambda_a r^4}{R^4}\right)\right]+r^2\frac{\partial W}{\partial E_{\theta\theta}}-\frac{\partial W}{\partial E_{rr}}-r\frac{d}{dr}\left(\frac{\partial W}{\partial E_{rr}}\right)+T_0\cos^2\alpha_f\right\}, \tag{17}$$

where

$$\frac{d}{dr}\left(\frac{\partial W}{\partial E_{rr}}\right)=k_{rr}\frac{d}{dE_{rr}}\left(\frac{E_{rr}}{(c_{rr}-|E_{rr}|)^3}\right).\frac{1}{2}\frac{d}{dr}\left[\frac{R^2}{\lambda_a^2r^2}-1\right]=\frac{k_{rr}}{2}.\frac{c_{rr}+2E_{rr}}{(c_{rr}-|E_{rr}|)^4}\left\{-2\left(\frac{R}{\lambda_a}\right)^2\frac{1}{r^3}+\frac{2R}{\lambda_a^2r^2}\frac{dR}{dr}\right\}$$

or

$$r\frac{d}{dr}\left(\frac{\partial W}{\partial E_{rr}}\right)=\frac{k_{rr}}{\lambda_a^2}.\frac{c_{rr}+2E_{rr}}{(c_{rr}-|E_{rr}|)^4}\left[\lambda_a-\left(\frac{R}{r}\right)^2\right].$$

To simplify (17), let

$$Q_1=1+\left(\frac{r\phi_a}{\lambda_a}\right)^2-\lambda_a^2\left(\frac{3r^2}{R^2}-\frac{2\lambda_a r^4}{R^4}\right) \qquad \text{(units: dimensionless)}$$

$$Q_2=r^2\frac{\partial W}{\partial E_{\theta\theta}}-\frac{\partial W}{\partial E_{rr}}=r^2\frac{k_{\theta\theta}.E_{\theta\theta}}{(c_{\theta\theta}-|E_{\theta\theta}|)^3}-\frac{k_{rr}.E_{rr}}{(c_{rr}-|E_{rr}|)^3} \qquad \text{(units: J.L}^{-1}\text{)}$$

$$Q_3=r\frac{d}{dr}\left(\frac{\partial W}{\partial E_{rr}}\right)=r\frac{d}{dr}\left(\frac{\partial W}{\partial E_{rr}}\right)=\frac{k_{rr}}{\lambda_a^2}.\frac{c_{rr}+2E_{rr}}{(c_{rr}-|E_{rr}|)^4}\left[\lambda_a-\left(\frac{R}{r}\right)^2\right] \qquad \text{(units: J.L}^{-1}\text{)}$$

Then (17) becomes

$$\frac{dp}{dr}=\frac{R^2}{r^3\lambda_a^2}\{pQ_1+Q_2-Q_3+T_0\cos^2\alpha_f\} \qquad \text{(units: J.L}^{-1}\text{.cm}^{-1}\text{)}$$

Zero traction boundary condition

The zero traction boundary condition $\hat{T}^{rr}\big|_{r=r_{epi}}=0$ at the outer radial surface provides the initial condition for solving (17):

$$\hat{T}^{rr}\big|_{r=r_{epi}}=\frac{\partial W}{\partial E_{rr}}\Big|_{r=r_{epi}}+p_{epi}\left(\frac{\lambda_a r_{epi}}{R_{epi}}\right)^2=0,$$

gives

$$p = p_{epi} = -\left(\frac{R_{epi}}{\lambda_a r_{epi}}\right)^2 \frac{\partial W}{\partial E_{rr}}\Big|_{r=r_{epi}} = -\left(\frac{R_{epi}}{\lambda_a r_{epi}}\right)^2 \frac{k_{rr}.E_{rr}^{epi}}{\left(c_{rr}-\left|E_{rr}^{epi}\right|\right)^3}.$$

Now using

$$s = \frac{r-r_{epi}}{r_{endo}-r_{epi}}, \quad \text{or} \quad r = r_{epi} + s\left(r_{endo} - r_{epi}\right),$$

we integrate (16) for $\hat{p} = p - p_{epi}$ from $s = 0$ ($r = r_{epi}$) to $s = 1$ ($r = r_{endo}$) with

$$\frac{d\hat{p}}{ds} = \left(r_{endo} - r_{epi}\right)\frac{R^2}{r^3\lambda_a^2}\left\{\left(\hat{p} + p_{epi}\right)\left[1 + \left(\frac{r\phi_a}{\lambda_a}\right)^2 - \lambda_a^2\left(\frac{3r^2}{R^2} - \frac{2\lambda_a r^4}{R^4}\right)\right] + r^2\frac{\partial W}{\partial E_{\theta\theta}} - \frac{\partial W}{\partial E_{rr}} - r\frac{d}{dr}\left(\frac{\partial W}{\partial E_{rr}}\right) + T_0\cos^2\alpha_f\right\}, \quad (18)$$

where the incompressibility condition (3) gives

$$r_{epi} = \sqrt{r_{endo}^2 + \frac{1}{\lambda_a}\left(R_{epi}^2 - R_{endo}^2\right)}$$

The solution yields a value of $p_{endo} = p_{epi} + \hat{p}|_{r=r_{endo}}$ which, with the first of (16), gives

$$p_{LV} = -\hat{T}^{rr}\Big|_{r=r_{endo}} = \frac{\partial W}{\partial E_{rr}}\Big|_{r=r_{endo}} + p_{endo}\left(\frac{\lambda_a r_{endo}}{R_{endo}}\right)^2 \quad (19)$$

Axial force and torque

In the analysis so far, the axial extension λ_a and axial twist ϕ_a have been specified, which requires the direct stress $T^{33} = T^{zz}$ and the shear stress $T^{32} = T^{z\theta}$ to be matched by corresponding boundary tractions in order to satisfy axial stress equilibrium. The radial distributions of these stresses, expressed as Cauchy stresses from (12), are:

$$\hat{T}^{zz} = \frac{k_{zz}E_{zz}}{(c_{zz}-|E_{zz}|)^3} + p\lambda_a^{-2} + T_0\sin^2\alpha_f, \qquad \text{where } E_{zz} = \lambda_a^2 + (r\phi_a)^2 - 1,$$

and

$$\hat{T}^{z\theta} = r\frac{k_{z\theta}E_{z\theta}}{(c_{z\theta}-|E_{z\theta}|)^3} + p\frac{r\phi_a}{\lambda_a^2} + T_0\cos\alpha_f\sin\alpha_f, \qquad \text{where } E_{z\theta} = \phi_a r^2.$$

Note that these stresses vary radially. Integrating over the area of the deformed cylinder at an axial (constant z) location gives the total axial force and torque:

$$f^{zz} = \int_{r_{endo}}^{r_{epi}} \hat{T}^{zz}\, 2\pi r.\, dr \quad \text{or} \quad \frac{d}{dr}f^{zz} = 2\pi r\hat{T}^{zz} \quad (20)$$

and

$$f^{z\theta} = \int_{r_{endo}}^{r_{epi}} \hat{T}^{z\theta}\, 2\pi r.\, dr \quad \text{or} \quad \frac{d}{dr}f^{z\theta} = 2\pi r\hat{T}^{z\theta}. \quad (21)$$

The axial extension λ_a and axial twist ϕ_a can now be chosen to make the net axial force and torque zero, but the zero-mean radially distributed boundary tractions are still needed to maintain the simple kinematics of the deforming cylinder.

Example solution

We illustrate the solution of the equations above under a specified loading condition with a linearly varying fibre orientation (α_f = +90deg to -60deg) and an active stress $T_0 = 1$. In the undeformed state, the cylinder has an inner radius of $R = 1$ and an outer radius of $R = 2$. The material parameters are all set with the poles at $c_{\alpha\beta} = 1.2$ (20% strain) and the scaling parameters at $k_{\alpha\beta} = 1$. These should of course be set to different values to reflect both the anisotropy of the myocardial tissue and the difference between tension and compression, and can also have transmurally varying values. Figure 9 shows the transmural ($1 \leq R \leq 2$) strain, stress and pressure distributions for a 20% radial expansion ($r_0 = 1.2$) with $\phi_a = 0$ (gives zero net torque) and $\lambda_a = 0.95$ (gives zero net axial force).

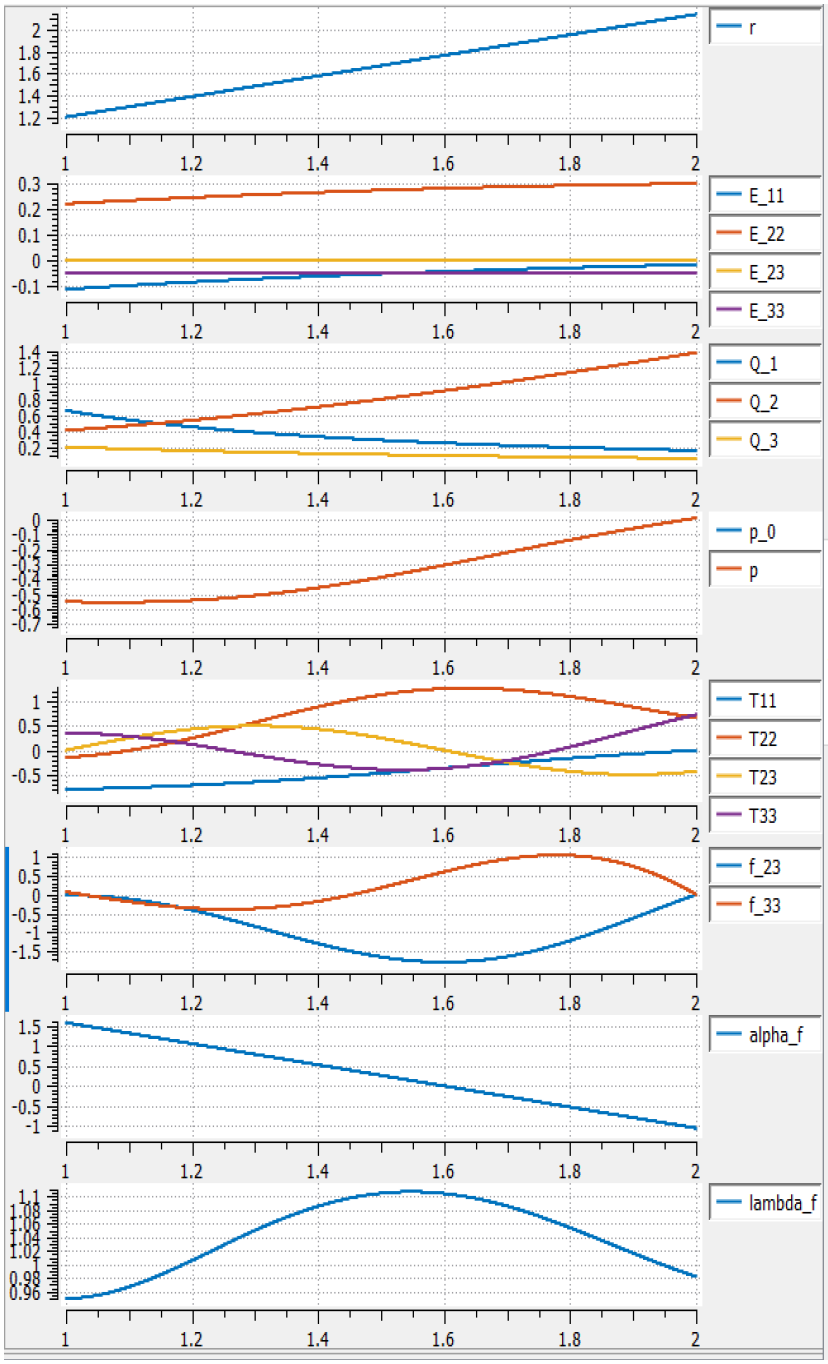

The radial coordinate in the deformed cylinder varies from the prescribed 1.2 (20% inflation) at the inner radius $R = 1$ to the calculated 2.15 at the outer $R = 2$.

The components of the Green strain tensor. Note that E_{33} is set by the prescribed constant value of $\lambda_a = 0.95$. The largest strain is the circumferential E_{22}. Note that the radial strain E_{11} is compressive.

These are intermediate quantities used in the differential equation for pressure.

p is the hydrostatic pressure, found by integrating a differential equation arising from radial stress equilibrium.

The components of the 2nd Piola-Kirchhoff stress tensor. Note that T^{11} is zero at the outer radial boundary and gives the cavity pressure (-0.8) at the inner radius. The axial stress T^{33} and shear stress T^{23} vary radially about a zero mean.

These show the intermediate results when integrating the axial stresses (from $R = 2$ to $R = 1$) to find the total axial force f^{33} and axial torque f^{23}. Note that λ_a and ϕ_a are chosen so that both f^{33} and f^{23} end up close to zero (see values at the inner radius).

The variation of muscle fibre angle α_f from 90deg at the inner radius to -60deg at the outer radius.

The fibre stretch λ_f. Note that λ_f at the inner radius is equal to the prescribed axial stretch $\lambda_a$because the fibre angle is aligned with the axial direction at this boundary.

Figure 9 Transmural distributions of strain and stress, etc, for $r_0 = 1.2$ with $\phi_a = 0$ and $\lambda_a = 0.95$. The radial coordinate in the undeformed cylinder varies from $R = 1$ to $R = 2$. All quantities shown are plotted against R.

Driving forces for LV volume change

Figure 10 illustrates the forces driving LV volume change during various phases of the cardiac cycle:

(a) Atrial systole.

In this phase the mitral value is open and the expansion of the LV FTU is driven by the small increase in LV pressure p_{LV} associated with LA contraction. A further equation is needed to link p_{LV} with atrial pressure p_{LA} and the flow through the mitral valve (v_{mitral}) that drives the change in LV volume $q_{LV} = \lambda_a \pi r_{endo}^2$:

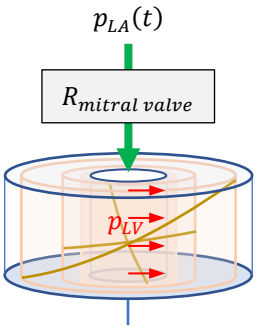

$$p_{LA} - p_{LV} = R_{mitral} . v_{mitral} \ ,$$

where R_{mitral} is the flow resistance of the mitral valve, and hence

$$\frac{d}{dt} q_{LV} = v_{mitral} = \frac{p_{LA} - p_{LV}}{R_{mitral}} \quad \text{and} \quad r_{endo} = \sqrt{\frac{q_{LV}}{\lambda_a \pi}} . \qquad (22)$$

FTU: The boundary condition is now $p_{LA}(t)$ and during the solution of equation 22 (in a python script), the current value of q_{LV} and hence r_{endo} is used in (18) and (19), with $T_0 = 0$, to return p_{LV}.

(b) Isovolumic contraction.

The rise in active myocyte tension (T_0) is initiated by electrical activation of the myocardium (the QRS complex of the ECG), calcium release and cross-bridge cycling. This rapidly raises p_{LV}, so that almost immediately the mitral valve closes and the LV undergoes a pressure rise under isovolumic conditions that ends when the aortic valve opens. The dominant force is now produced in the fibre directions by active myofilament contraction.

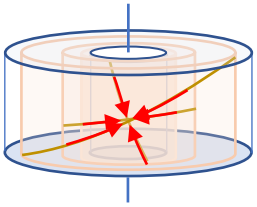

FTU: r_0 fixed; $T_0 > 0$; p_{LV} computed.

(c) Ventricular systole.

When $p_{LV} > p_{aorta}$, the LV ejects blood. Systole ends when mechanical feedback from the deforming tissue causes Ca^{2+} to detach from TnC to remove cross-bridge access to sites on the actin filament, so that T_0 drops and p_{LV} begins to drop. This phase also needs an additional equation relating LV volume change ($\frac{d}{dt} q_{LV}$) to the flow ($v_{aortic\ valve}$) through the aortic valve

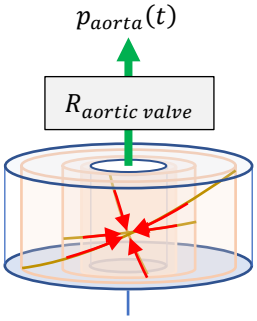

$$p_{LV} - p_{aorta} = R_{aortic\ valve} . v_{aortic\ valve} \ ,$$

where $R_{aortic\ valve}$ is the flow resistance of the aortic valve, and hence

$$\frac{d}{dt} q_{LV} = v_{aortic\ valve} = \frac{p_{LV} - p_{aorta}}{R_{aortic\ valve}} \quad \text{and} \quad r_{endo} = \sqrt{\frac{q_{LV}}{\lambda_a \pi}} . (22)$$

FTU: The boundary condition is now $p_{aorta}(t)$; $T_0 > 0$.

(d) Isovolumic relaxation.

When $p_{LV} < p_{aorta}$ the aortic valve closes and p_{LV} falls rapidly under isovolumic conditions.

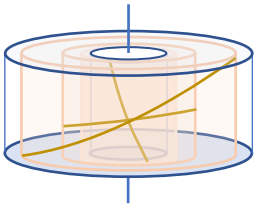

FTU: r_0 fixed; $T_0 = 0$; p_{LV} computed.

(e) <u>Rapid LV filling</u>.

When $p_{LV} < p_{LA}$ the mitral valve opens. The stored elastic energy drives expansion and inflow from the LA using equation 22.

FTU: The boundary condition is now $p_{LA}(t)$; $T_0 = 0$.

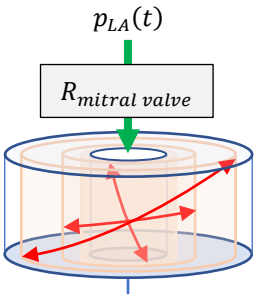

These 5 phases of the cardiac cycle are shown in Figure 10 relative to other cardiac events.

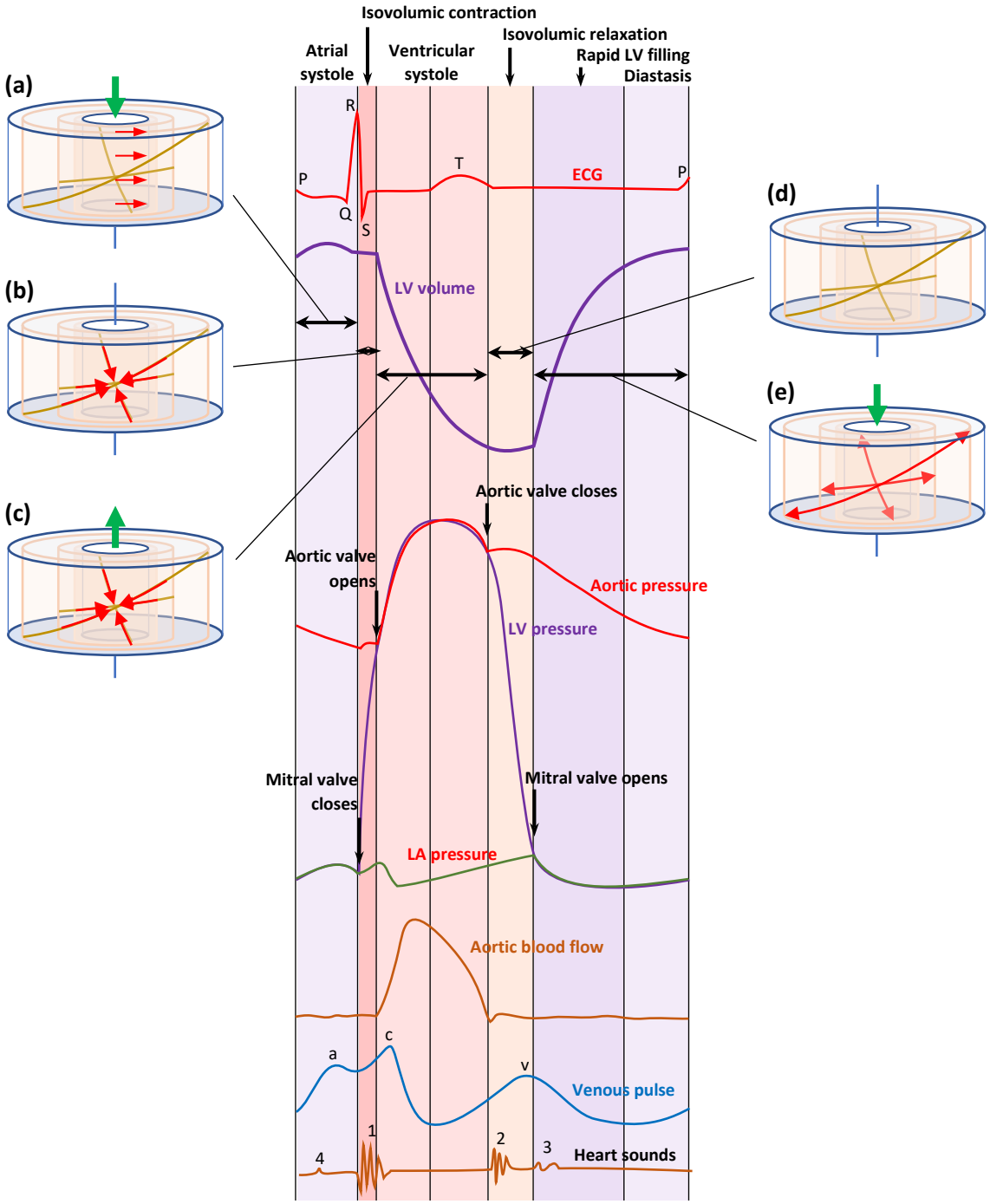

Figure 10 The key events in the cardiac cycle. (a) .. (d) indicate the driving forces on the LV FTU during four phases of the cardiac cycle: atrial systole, ventricular systole, isovolumetric relaxation, and ventricular filling.

Relating deformation of cylinder to deformation of the left ventricle

One strategy would be to link the cylinder deformation with a PCA mode of ventricular deformation.

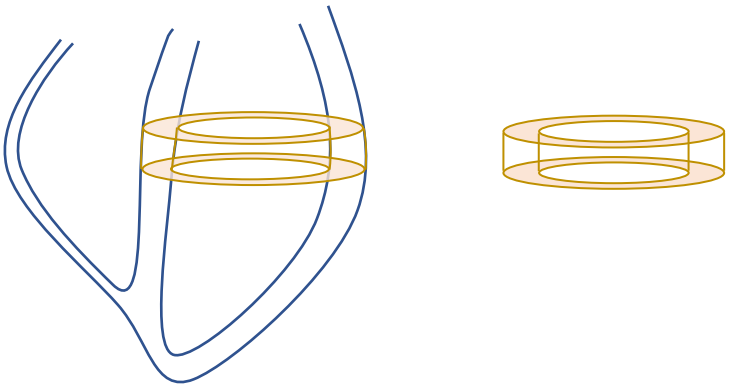

Active tension T_0 can be defined by the HMT model as follows.

6.6 Myofilament mechanics

We first present a constitutive model for isometric tension, the so-called *fading-memory model* that captures the key features of muscle fibre dynamics (including an explicit reproduction of the classic Hill force-velocity relation), and then a model of calcium activation of the cross-bridges.

Isometric tension-length-Ca^{2+} relation

The deformed length of a muscle fibre divided by its undeformed length is denoted by the muscle stretch λ. The muscle tension developed at a fixed λ is called the *isometric tension* $T_0(\lambda)$. Since this has a dependence on the level of intracellular calcium $[Ca^{2+}]_i$, we refer to $T_0(\lambda, [Ca^{2+}]_i)$ as the *isometric tension-length-Ca^{2+} relation* - see Figure 6.6.1, which also illustrates the relationship with the passive tension-length relation $T_p(\lambda)$.

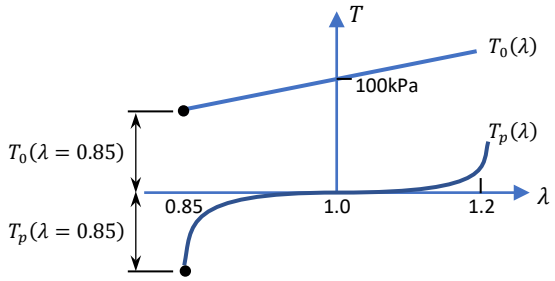

Figure 6.6.1 The active and passive isometric tension-length relations for a skeletal muscle fibre.

Fading memory model of muscle fibre mechanics

Dynamic length changes in a muscle fibre are small in comparison to the corresponding changes in tension. For example, a sudden length change of less than 1% causes muscle tension to fall by 100%. But the relationship between muscle fibre tension and the velocity of steady shortening, for example, is characteristically highly non-linear. We therefore propose that some (as yet unspecified) static nonlinear function of tension, $Q(T, T_0)$, can be expressed as a linear superposition of dynamic length changes:

$$Q(T, T_0) = \int_{-\infty}^{t} \Phi(t - \tau)\dot{\lambda}(\tau)d\tau \ ,$$

where $\dot{\lambda} = \frac{d\lambda}{dt}$ is the muscle fibre velocity (s^{-1}), and $\Phi(t) = \sum_i A_i\, e^{-\alpha_i t}$ is a material response function that is expressed as a sum of exponential decay terms (since memory 'fades' – recent events are more significant than older events):

$$Q(T, T_0) = \sum_i A_i \int_{-\infty}^{t} e^{-\alpha_i (t-\tau)}\, \dot{\lambda}(\tau) d\tau \qquad (6.6.1)$$

Under steady state conditions the RHS of (6) is zero and the function $Q(T, T_0)$ must be defined such that $Q(T_0, T_0) = 0$. A system defined by (6) is known in the system identification literature as a `Wiener cascade model' - a linear dynamic system followed by a static nonlinearity.

Two further experimental observations can now be used. The first is that all tension measurements on muscle scale with the isometric tension and therefore $Q(T, T_0) = Q(T/T_0)$. The second is that tension recovery following a step change in length shows evidence of three distinct physical processes: the initial fast recovery with a slight oscillation is indicative of a second order process (e.g. myosin head rotation in the model by Huxley and Simmons, 1971) and the subsequent slow recovery phase is evidence of a first order process (the crossbridge detachment/attachment cycle in the Huxley, 1957, model with the rate limiting step being detachment). We therefore limit the number of rate constants to 3 and (6) becomes

$$Q(T/T_0) = \sum_{i=1,3} A_i \int_{-\infty}^{t} e^{-\alpha_i (t-\tau)}\, \dot{\lambda}(\tau) d\tau \qquad (6.6.2)$$

where α_1 is the rate constant associated with the first order slow tension recovery, and α_2 and α_3 are the rate constants for the second order fast recovery process in Figure 6.6.2(a).

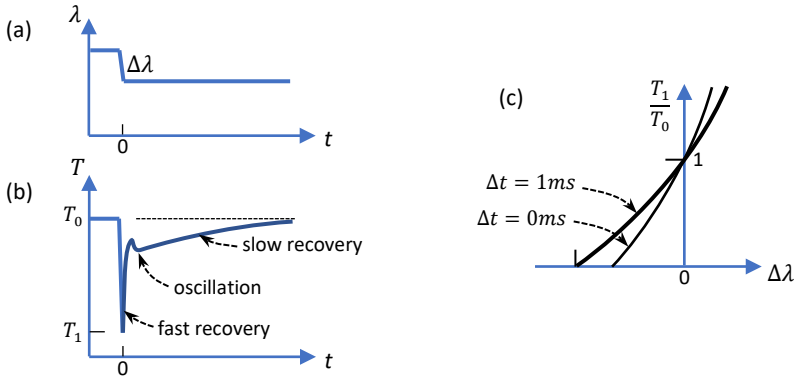

Figure 6.6.2 Tension response to a rapid shortening step (magnitude $\Delta\lambda$ and duration Δt). The tension drops almost instantaneously from the isometric tension T_0 to a post-step value T_1 before a fast recovery phase, an oscillatory phase, and then a slow recovery to the isometric value for the new length.

A third experimental observation, on the relationship between the constant muscle shortening velocity and a constant load, is now used to determine the functional form of $Q(T/T_0)$.

Constant velocity experiments

A parameterised form of the nonlinear $Q(T/T_0)$ function can be determined from constant velocity experiments. In these experiments the muscle is servo-controlled to shorten at a constant rate, or shortens at a constant rate (following an initial transient) in response to a reduction in tension to a constant value less than T_0. The plot of tension versus velocity is called a force/velocity curve. These curves are typically hyperbolic and are accurately described for tetanised (maximally activated) muscle by the equation first proposed by Hill (1938):

$$\frac{-V}{aV_0} = \frac{\dot{\lambda}}{aV_0} = \frac{T_1/T_0 - 1}{T_1/T_0 + a}$$

where V_0 is the maximum velocity (achieved when $T = 0$) and a is a parameter which controls the curvature of the force/velocity relation (the parameter a here is chosen to be non-dimensional, the a in Hill's original equation is equivalent here to aT_0). As with force recovery following a length step, the force/velocity curves scale with isometric tension T_0.

The unloaded shortening velocity V_0 has had a special significance for muscle physiologists because it appeared to be independent of length and level of activation, at least for lengths greater than resting length ($\lambda > 1$). For $\lambda < 1$ the passive muscle structures are in compression and the `unloaded' shortening is then shortening against an internal load.

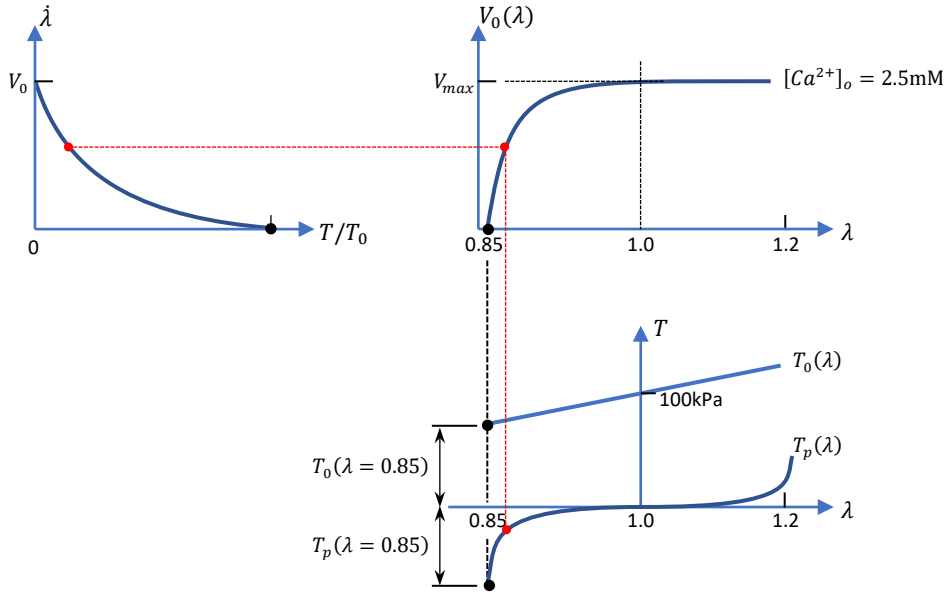

Figure 6.6.3

Ignoring the two rate constants α_2, α_3 associated with the initial transient following the tension step (since this has decayed by the time the force/velocity measurements are made) and putting $\dot{\lambda} = -V$ (the constant velocity of shortening), (5.8.2) reduces to $Q(T/T_0) = -A_1 V/\alpha_1$. An exact match to Hill's force/velocity relation [Hill, 1938] is then obtained by choosing $Q(T/T_0) = \frac{T/T_0 - 1}{T/T_0 + a}$ and $V_0 = \alpha_1/aA_1$, giving

$$\dot{\lambda} = -V = \frac{\alpha_1}{A_1}\frac{T/T_0 - 1}{T/T_0 + a}. \qquad (6.6.3)$$

The fading memory model of crossbridge mechanics is now given by

$$\frac{T/T_0 - 1}{T/T_0 + a} = \sum_{i=1}^{3} A_i \int_{-\infty}^{t} e^{-\alpha_i(t-\tau)}\, \dot{\lambda}(\tau) d\tau$$

or

$$T = T_0 \frac{1 + aQ}{1 - Q}, \text{ where } Q = \sum_{i=1}^{3} A_i \int_{-\infty}^{t} e^{-\alpha_i(t-\tau)}\, \dot{\lambda}(\tau) d\tau \qquad (6.6.4)$$

Note that if length changes are relatively slow, one rate constant is sufficient and (9), using the Leibnitz formula for differentiating an integral, reduces to

$$T = T_0 \frac{1 + aQ}{1 - Q},$$

where

$$\frac{dQ}{dt} = -\alpha_1 Q + A_1 \dot{\lambda}. \qquad (6.6.5)$$

Calcium binding and cross-bridge activation

Calcium attaching to troponin C changes the molecular structure of tropomyosin such that sites on the thin filiament that were previously blocked, become available for cross-bridge head binding and tension development. The fraction of actin sites available for cross-bridge binding (denoted by *z*) is given by the following first order equation:

$$\frac{dz}{dt} = \alpha_0 \left[\left(\frac{[Ca]_b}{[Ca]_{50}} \right)^n . (1 - z) - 1 \right], \qquad (6.6.6)$$

where $[Ca]_b$ is the concentration of bound calcium, $[Ca]_{50}$ is the concentration at which 50% of the available troponin C sites are occupied by calcium, and α_0 is the rate constant for calcium binding.

$$\frac{d[Ca]_b}{dt} = \rho_0 [Ca]_i . \left([Ca]_{b_{max}} - [Ca]_b \right)$$

Coupling to the cardiovascular system

Let v be volumetric flow rate in m^3 or L, with co-energy potential u in $J.m^{-3}$ or $J.L^{-3}$ (the fluid pressure).

Elastic storage in a compliant vessel is $q = \int v dt$ where v is the net flow into the elastic segment and q (m^3) is the excess volume caused by dilation of that segment (see Figure 4.3.3). For flow through a vessel of length l, radius r, and wall thickness h, the elasticity of the wall assuming a linear elastic material with modulus E, is $\frac{Eh}{2\pi r^3 l}$. Inertial storage is $L\dot{v}$, where $L = \frac{\rho l}{\pi r^2}$ (Js^2m^{-6}), and the constitutive relation for resistance or dissipation is given by the Poiseuille relation: $\Delta u = \mathrm{R}.v$, where $\mathrm{R} = \frac{8\eta l}{\pi r^4}$ ($Js.m^{-6}$) is the resistance to axial flow (of viscosity η).

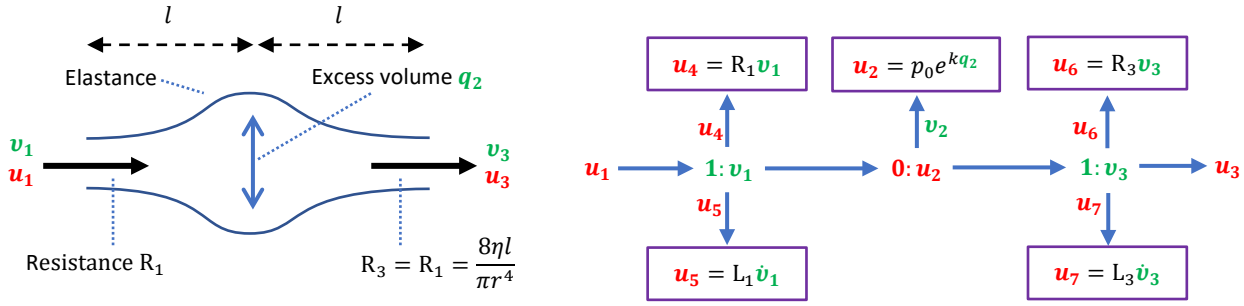

Figure 4.3.3 Bond graph model of Poiseuille flow through a compliant blood vessel. Note that the central 0: u_2 node imposes flow conservation that includes the vessel compliance. The two nodes 1: v_1 and 1: v_3 link in the energy associated with dissipative resistance for Poiseuille flow and inertial resistance to flow.

There are 10 state variables (v_1-v_3, u_1-u_7) with three conservation equations:

$$u_1 = u_2 + u_4 + u_5; \quad u_2 = u_3 + u_6 + u_7; \quad v_1 = v_2 + v_3;$$

and the five constitutive laws, shown in the boxes on the right in Figure 4.8. Two boundary conditions are therefore needed, such as the upstream flow v_1 and the downstream pressure u_3.

Note that the Laplace relation gives wall hoop stress $T = \frac{r}{h} u_2$, where r is vessel radius and h is wall thickness. The pressure u_2 is a nonlinear function of excess volume q_2: $u_2 = u_0 e^{kq_2}$, where u_0 is the pressure when $q_2 = 0$.

Refer to NS and include advective acceleration term.

Branching blood vessel

Flow through the flow bifurcation shown on the left in Figure 4.3.4 is represented by the bond graph model on the right. Inertial terms are omitted in this example but could be added to the 1:nodes as in Figure 4.3.3.

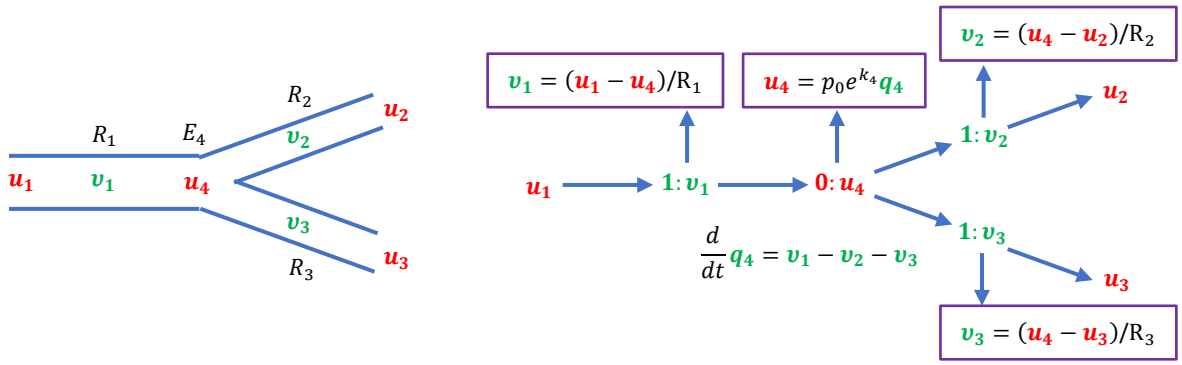

Figure 4.3.4 Bond graph model of a branching vessel. Note that the compliance for the junction is associated with the 0:node at the bifurcation point, while the resistances of the parent (R_1) and child branches (R_2 and R_3) are associated with 1:node flow terms.

Coupling cardiac FTU to CV system

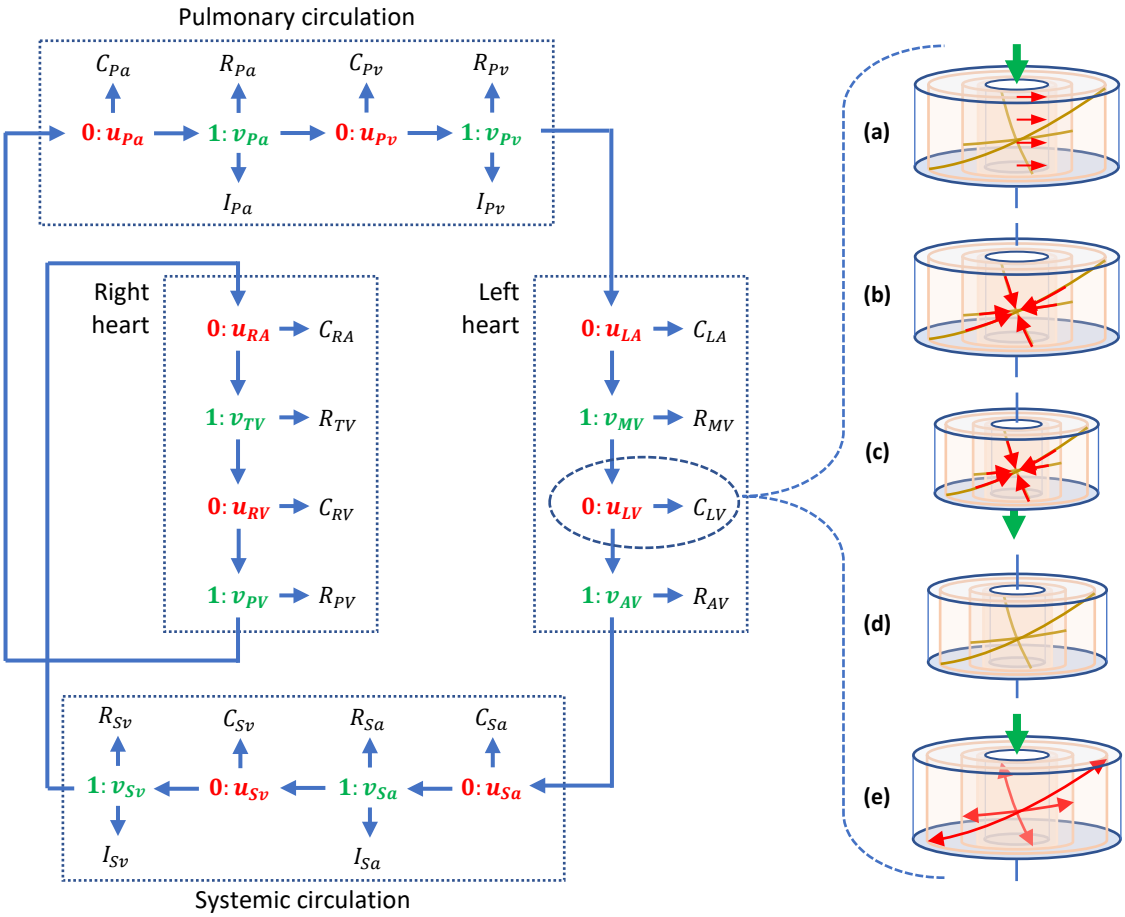

$$u_1 = u_2 + u_4 + u_5; \quad u_2 = u_3 + u_6 + u_7; \quad v_1 = v_2 + v_3;$$

Mass conservation

$0: u_{LA}$	$\frac{d}{dt} q_{LA} = v_{Pv} - v_{MV}$	where $u_{LA} = q_{LA}/C_{LA}$	$C_{LA} =$ ($L^2J^{-1}s^{-1}$)
$0: u_{LV}$	$\frac{d}{dt} q_{LV} = v_{MV} - v_{AV}$	where $u_{LV} = q_{LV}/C_{LV}$	$C_{LV} =$ ($L^2J^{-1}s^{-1}$)
$0: u_{Sa}$	$\frac{d}{dt} q_{Sa} = v_{AV} - v_{Sa}$	where $u_{Sa} = q_{Sa}/C_{Sa}$	$C_{Sa} =$ ($L^2J^{-1}s^{-1}$)
$0: u_{Sv}$	$\frac{d}{dt} q_{Sv} = v_{Sa} - v_{Sv}$	where $u_{Sv} = q_{Sv}/C_{Sv}$	$C_{Sv} =$ ($L^2J^{-1}s^{-1}$)
$0: u_{RA}$	$\frac{d}{dt} q_{RA} = v_{Sv} - v_{TV}$	where $u_{RA} = q_{RA}/C_{RA}$	$C_{RA} =$ ($L^2J^{-1}s^{-1}$)
$0: u_{RV}$	$\frac{d}{dt} q_{RV} = v_{TV} - v_{PV}$	where $u_{RV} = q_{RV}/C_{RV}$	$C_{RV} =$ ($L^2J^{-1}s^{-1}$)
$0: u_{Pa}$	$\frac{d}{dt} q_{Pa} = v_{PV} - v_{PA}$	where $u_{Pa} = q_{Pa}/C_{Pa}$	$C_{Pa} =$ ($L^2J^{-1}s^{-1}$)
$0: u_{Pv}$	$\frac{d}{dt} q_{Pv} = v_{Pa} - v_{Pv}$	where $u_{Pv} = q_{Pv}/C_{Pv}$	$C_{Pv} =$ ($L^2J^{-1}s^{-1}$)

Note: $\frac{d}{dt}(q_{LA} + q_{LV} + q_{Sa} + q_{Sv} + q_{RA} + q_{RV} + q_{Pa} + q_{Pv}) = 0$

Energy conservation

$1: v_{MV} \quad \boldsymbol{u_{LA}} = \boldsymbol{u_{LV}} + R_{MV}\boldsymbol{v_{MV}}$

$1: v_{AV} \quad \boldsymbol{u_{LV}} = \boldsymbol{u_{Sa}} + R_{AV}\boldsymbol{v_{AV}}$

$1: v_{Sa} \quad \boldsymbol{u_{Sa}} = \boldsymbol{u_{Sv}} + R_{Sa}\boldsymbol{v_{Sa}}$

$1: v_{Sv} \quad \boldsymbol{u_{Sv}} = \boldsymbol{u_{RA}} + R_{Sv}\boldsymbol{v_{Sv}}$

$1: v_{TV} \quad \boldsymbol{u_{RA}} = \boldsymbol{u_{RV}} + R_{TV}\boldsymbol{v_{TV}}$

$1: v_{PV} \quad \boldsymbol{u_{RV}} = \boldsymbol{u_{Pa}} + R_{PV}\boldsymbol{v_{PV}}$

$1: v_{Pa} \quad \boldsymbol{u_{Pa}} = \boldsymbol{u_{Pv}} + R_{Pa}\boldsymbol{v_{Pa}}$

$1: v_{Pv} \quad \boldsymbol{u_{Pv}} = \boldsymbol{u_{LA}} + R_{Pv}\boldsymbol{v_{Pv}}$

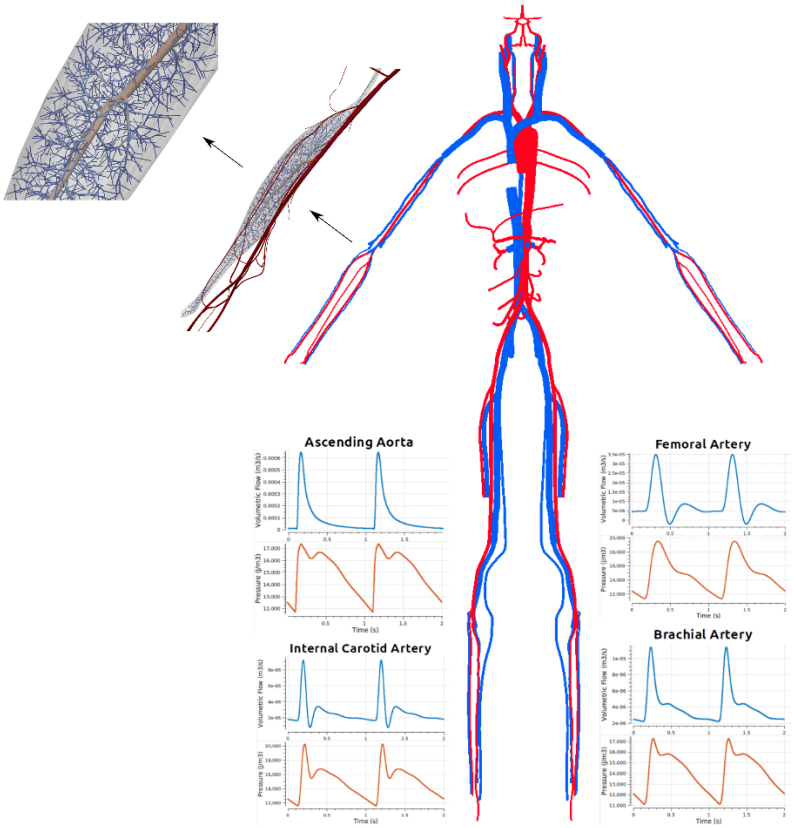

Figure 15. Cardiovascular system formulated with bond graph equations to ensure mass balance and energy balance. The major blood vessels (arteries and veins) are described discretely in relation to anatomical body coordinates. These are then coupled with organ-specific circulation models (shown here for one muscle) that are generated algorithmically for each organ. The whole body models run in real time on a laptop (pressure and flow solutions at a few points are shown).

References

1. Malvern, LE. Introduction to the mechanics of a continuous medium. Prentice-Hall 1969; p 667.